REPORT DOCUMENTATION PAGE			Form Approved OMB No. 0704-0188

1. REPORT DATE *(DD-MM-YYYY)* 10-4-2012	**2. REPORT TYPE** Technical Paper	**3. DATES COVERED** *(From - To)* 2010-2011
4. TITLE AND SUBTITLE Non-linear Dielectrics and Ferrites in ICEPIC		**5a. CONTRACT NUMBER** In-House
		5b. GRANT NUMBER
		5c. PROGRAM ELEMENT NUMBER 62605F
6. AUTHOR(S) Andrew D. Greenwood, David M. French, Brad W. Hoff, Susan L. Heidger		**5d. PROJECT NUMBER**
		5e. TASK NUMBER D01K
		5f. WORK UNIT NUMBER PPM 00001000 DF702172
7. PERFORMING ORGANIZATION NAME(S) AND ADDRESS(ES) Air Force Research Laboratory 3550 Aberdeen Avenue SE Kirtland AFB, NM 87117-5776		**8. PERFORMING ORGANIZATION REPORT NUMBER**
9. SPONSORING / MONITORING AGENCY NAME(S) AND ADDRESS(ES) Air Force Research Laboratory 3550 Aberdeen Avenue SE Kirtland AFB, NM 87117-5776		**10. SPONSOR/MONITOR'S ACRONYM(S)** AFRL/RDHE
		11. SPONSOR/MONITOR'S REPORT NUMBER(S) AFRL-RD-PS-TP-2013-0005

12. DISTRIBUTION / AVAILABILITY STATEMENT
Approved for public release; distribution unlimited.

13. SUPPLEMENTARY NOTES
377ABW-2011-1683; 21 December 2011

28th International Review of Progress in Applied Computational Electromagnetics

Government Purpose Rights

14. ABSTRACT
Models for non-linear dielectrics and magnetic ferrites are developed and coded into the particle-in-cell code ICEPIC. The non-linear dielectric model includes a relaxation term to account for the physical response time of the material, which may be longer than an FDTD time step. The ferrite model accounts for the non-linearity of the Landau-Lifshitz-Gibert equation, and the magnetization update is derived from the solution of the equation on a time step. Initial testing of the models is encouraging, and work is underway on further improvement and refinement.

15. SUBJECT TERMS
FDTD, non-linear

16. SECURITY CLASSIFICATION OF:			**17. LIMITATION OF ABSTRACT**	**18. NUMBER OF PAGES**	**19a. NAME OF RESPONSIBLE PERSON** Andrew Greenwood
a. REPORT UNCLASS	**b. ABSTRACT** UNCLASS	**c. THIS PAGE** UNCLASS	SAR	5	**19b. TELEPHONE NUMBER** *(include area code)* 505-846-6642

Non-linear Dielectrics and Ferrites in ICEPIC

Andrew D. Greenwood, David M. French, Brad W. Hoff, Susan L. Heidger

Air Force Research Laboratory, Directed Energy Directorate, Kirtland AFB, NM 87117-5776 USA
agreenwood@ieee.org

Abstract: Models for non-linear dielectrics and magnetic ferrites are developed and coded into the particle-in-cell code ICEPIC. The non-linear dielectric model includes a relaxation term to account for the physical response time of the material, which may be longer than an FDTD time step. The ferrite model accounts for the non-linearity of the Landau-Lifshitz-Gibert equation, and the magnetization update is derived from the solution of the equation on a time step. Initial testing of the models is encouraging, and work is underway on further improvement and refinement.

Keywords: FDTD, non-linear

1. Introduction

The improved concurrent electromagnetic particle-in-cell (ICEPIC) code implements finite-difference time-domain (FDTD) electromagnetics and the relativistic Lorentz force law for tracking charged particles. The code is massively parallel and applicable to modeling a variety of high power microwave (HPM) devices [1], [2]. More recently, there is interest in the use of non-linear materials in the generation of HPM. Two types of materials are of interest, non-linear dielectric materials and ferrite materials, which are governed by the Landau-Lifshitz-Gilbert equation. Although previous authors consider similar materials [3]–[6], to our knowledge, aspects of our formulation and concerns related to the generation of high power microwaves are unique.

2. Formulation

A. Non-linear Dielectrics

Non-linear dielectrics are materials for which the permittivity depends on the electric field strength. Of particular interest are materials for which the permittivity is a decreasing function of the electric field. In such materials, higher field values experience lower permittivity, hence faster wave propagation speed. This leads to a steepening of a wave pulse as it propagates, or in other words, the formation of a shock wave.

The approach to modeling non-linear dielectric material is to curve fit an analytical function to experimental permittivity data. Two fitting functions considered are the Lorentzian function, given by

$$\epsilon_r(E) = \frac{A}{\pi} \frac{0.5\Gamma}{(E - E_0)^2 + (0.5\Gamma)^2} \tag{1}$$

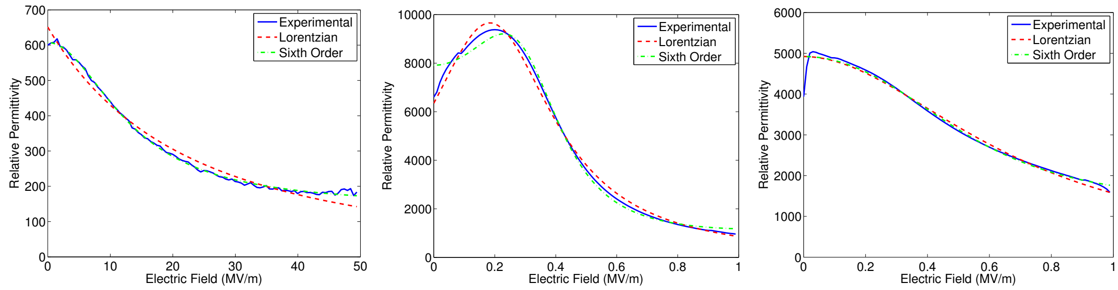

(a) Barium Strontium Titanate (b) Lead Magnesium Niobate 38 (c) Lead Magnesium Niobate 85

Figure 1: Experimental relative permittivity and associated curve fits for materials of interest.

where A, E_0, and Γ are parameters of the fit. The primary disadvantage to the Lorentzian function is $\epsilon_r(E \to \infty) \to 0$; permittivity values below one are problematic. Thus, the second (sixth order) fitting function, given by

$$\epsilon_r(E) = \epsilon_{r,\infty} + \frac{\epsilon_{r,0} - \epsilon_{r,\infty}}{1 + a_1 E^2 + a_2 E^4 + a_3 E^6} \tag{2}$$

where $\epsilon_{r,\infty}$, $\epsilon_{r,0}$, a_1, a_2, and a_3 are parameters of the fit. For this function, $\epsilon_r(0) = \epsilon_{r,0}$ and $\epsilon_r(E \to \infty) \to \epsilon_{r,\infty}$. Plots of experimental data and associated curve fits for three materials of interest are shown in Fig. 1. Note that in addition to being non-linear, the permittivity values in these materials are quite large.

The incorporation of the non-linear permittivity into Maxwell's equations involves the interpolation of the staggered electric field values from the previous time step to find the magnitude of E at a given field point, then the computation of the permittivity based on E. The computed permittivity is then used to update first $\mathbf{D}$, then $\mathbf{E}$ from Ampere's law and from $\mathbf{D} = \epsilon\mathbf{E}$. For stability, it is important that only past values of E contribute to the computed permittivity [7].

The physical response time of a material is often much slower than an FDTD time step. Thus, in the formulation, the response of the material is incorporated using

$$\alpha \frac{\partial \epsilon_r}{\partial t} + \epsilon_r = f(E) \tag{3}$$

where $f(E)$ is $\epsilon_r(E)$ from Eq. 1 or 2. Analytically solving this equation on a time step yields

$$\begin{aligned}\epsilon_r^n = \epsilon_r^{n-1} e^{-\alpha\Delta_t} + \left[f(E^{n-1}) - \alpha \left.\frac{\partial f}{\partial E}\right|_{E^{n-1}} \frac{E^{n-1} - E^{n-2}}{\Delta_t} \right] \left[1 - e^{-\alpha\Delta_t}\right] \\ + \Delta_t \left.\frac{\partial f}{\partial E}\right|_{E^{n-1}} \frac{E^{n-1} - E^{n-2}}{\Delta_t}\end{aligned} \tag{4}$$

B. Magnetic Ferrites

In many cases, a ferrite can be modeled by assuming a large, static magnetic field and forming a linearized gyrotropic permeability [8]. However, the applications of interest do not admit such a model. Thus, the magnetization is modeled using the Landau-Lifshitz-Gilbert equation,

$$\frac{\partial \mathbf{M}}{\partial t} = -\frac{\gamma_0}{1+\lambda^2}\left(\mathbf{M}\times\mathbf{H}_{\text{eff}} + \frac{\lambda}{|\mathbf{M}|}\mathbf{M}\times\mathbf{M}\times\mathbf{H}_{\text{eff}}\right) \tag{5}$$

where $\gamma_0 = 2.212761045\times 10^5 \text{m}/(\text{A s})$,

$$\mathbf{H}_{\text{eff}} = \mathbf{H} + \mathbf{H}_{\text{static}} - \frac{2k_u}{\mu_0|\mathbf{M}|^2}\left(\mathbf{M}\cdot\hat{u}\right)\hat{u} + \frac{2A}{\mu_0|\mathbf{M}|^2}\nabla^2\mathbf{M} \tag{6}$$

$$\mathbf{B} = \mu_0\left(\mathbf{H}+\mathbf{M}\right) \tag{7}$$

and $|\mathbf{M}| = M_s$, λ (sometimes denoted α), k_u, $\hat{u}$, and A are parameters of the material being modeled. Note that Eq. 5 keeps the magnitude of $\mathbf{M}$ constant with time but varies its direction.

Ferrite materials are modeled by placing all components of the magnetization vector ($\mathbf{M}$) at the center of a FDTD cell. The magnetic field values are interpolated from the staggered Yee grid to the center of the cell, and the quantity $\bar{\mathbf{H}}_{\text{eff}} = \mathbf{H}_{\text{eff}} + (\lambda/|\mathbf{M}|)\mathbf{M}\times\mathbf{H}_{\text{eff}}$ is defined. Eq. 5 then becomes

$$\frac{\partial \mathbf{M}}{\partial t} = -\frac{\gamma_0}{1+\lambda^2}\mathbf{M}\times\bar{\mathbf{H}}_{\text{eff}} \tag{8}$$

which can be solved on $t = [(n-0.5)\Delta_t, (n+0.5)\Delta_t)$ to give

$$\begin{aligned}\mathbf{M}^{n+0.5} = &\frac{\left(\mathbf{M}^{n-0.5}\cdot\bar{\mathbf{H}}^n_{\text{eff}}\right)\bar{\mathbf{H}}^n_{\text{eff}}}{|\bar{\mathbf{H}}^n_{\text{eff}}|^2} \\ &+\left(\mathbf{M}^{n-0.5} - \frac{\left(\mathbf{M}^{n-0.5}\cdot\bar{\mathbf{H}}^n_{\text{eff}}\right)\bar{\mathbf{H}}^n_{\text{eff}}}{|\bar{\mathbf{H}}^n_{\text{eff}}|^2}\right)\cos\left(\frac{\gamma_0}{2(1+\lambda^2)}|\bar{\mathbf{H}}^n_{\text{eff}}|\Delta_t\right) \\ &-\frac{\mathbf{M}^{n-0.5}\times\bar{\mathbf{H}}^n_{\text{eff}}}{|\bar{\mathbf{H}}^n_{\text{eff}}|}\sin\left(\frac{\gamma_0}{2(1+\lambda^2)}|\bar{\mathbf{H}}^n_{\text{eff}}|\Delta_t\right)\end{aligned} \tag{9}$$

In practice, $\bar{\mathbf{H}}^n_{\text{eff}}$ is approximated with $\bar{\mathbf{H}}^{n-0.5}_{\text{eff}}$. $\mathbf{B}$ is updated using Faraday's law, then the $\mathbf{M}$ values are interpolated to the $\mathbf{H}$ locations, and $\mathbf{H}$ is updated from Eq. 7.

3. Results

The dielectric model is tested by simulating a parallel plate capacitor filled with non-linear dielectric. A known current is driven from one plate to the other, and the electric field between the plates is observed. From Gauss' law, if A is the area of the plates, respectively, the current from one plate to the other is given by

$$i = \frac{dq}{dt} = A\frac{\partial}{\partial t}\left[\epsilon(E)E\right] \tag{10}$$

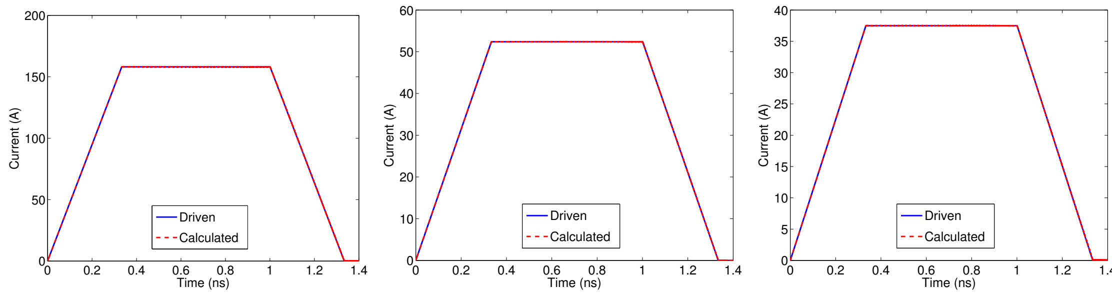

(a) Barium-Strontium-Titanate (b) Lead-Magnesium-Niobate 38 (c) Lead-Magnesium-Niobate 85

Figure 2: Comparison of computed current to drive current for parallel plate capacitor filled with three different non-linear dielectrics. For this test, the plate area is 2.5 mm^2, the plate separation is 0.632mm, and $\alpha = 10$ps.

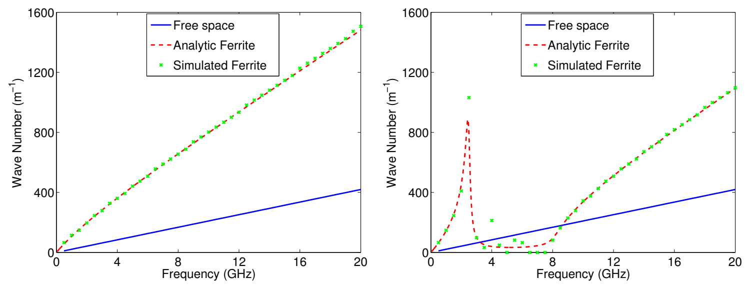

(a) Parallel propagation, lhc-pol (b) Parallel propagation, rhc-pol

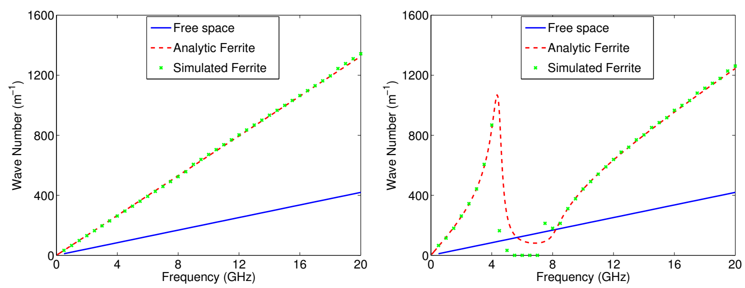

(c) Perpendicular propagation, parallel magnetic-pol (d) Perpendicular propagation, perpendicular magnetic-pol

Figure 3: Propagation characteristics for a $\epsilon_r = 10$, $\sigma = 0$, $M_s = 159$kA/m, $\lambda = 0.05$, $k_u = 0$, $A = 0$ ferrite in a 71.0kA/m static magnetic field.

The current computed from Eq. 10 is compared to the drive current. Results are shown in Fig. 2, and the agreement is good.

The ferrite model is tested by evaluating wave propagation in a ferrite in a large static magnetic field. In this regime, the ferrite behaves as a linearized gyrotropic material, and the wave number can be analytically computed [8]. Analytic and simulated wave number versus frequency plots are shown in Fig. 3 for a ferrite with $\epsilon_r = 10$, $\sigma = 0$, $M_s = 159$kA/m, $\lambda = 0.05$, $k_u = 0$, $A = 0$ in a 71.0kA/m static magnetic field. Results are shown for left-hand and right-hand circular polarization when the propagation is parallel to the magnetic field, and for the magnetic field polarized parallel and perpendicular to the static magnetic field when the propagation is perpendicular to the static field. Except when the attenuation of the ferrite is large (2-8 GHz for the right-hand circular

polarized case and 4-8 GHz for the perpendicular polarized case), the agreement is excellent.

In both models, a slow growth mode is sometimes observed. Investigation shows that the growth is related to aliasing when the wave number becomes larger than the Nyquist cut-off of the numerical grid. Work is underway to improve the utility of the models by suppressing this mode [9]. Results are to be reported in the conference presentation.

4. Conclusion

Models for non-linear dielectrics and magnetic ferrites are developed and coded into the particle-in-cell code ICEPIC. The non-linear dielectric model includes a relaxation term to account for the physical response time of the material, which may be longer than an FDTD time step. The ferrite model accounts for the non-linearity of the Landau-Lifshitz-Gibert equation, and the magnetization updated is derived from the solution of the equation on a time step. Initial testing of the models is encouraging, and work is underway on further improvement and refinement.

References

[1] R. E. Peterkin and J. W. Luginsland, "A virtual prototyping environment for directed-energy concepts," Comp. in Sci. and Eng., vol. 4, pp. 42–49, 2002.

[2] M. Bettencourt and A. Greenwood, "Performance improvements for efficient electromagnetic particle-in-cell computation on 1000s of cpus," IEEE Trans. Antennas Propagat., vol. 56, pp. 2178 –2186, 2008.

[3] R. M. Joseph and A. Taflove, "FDTD Maxwell's equations models for nonlinear electrodynamics and optics," IEEE Trans. Antennas Propagat., vol. 45, pp. 364 –374, 1997.

[4] M. Slodicka and L. Banas, "A numerical scheme for a Maxwell-Landau-Lifshitz-Gilbert system," Applied Mathematics and Computation, vol. 158, pp. 79 –99, 2004.

[5] M. Lakshmanan, "The fascinating world of the Landau-Lifshitz-Gilbert equation: an overview," Phil. Trans. R. Soc. A, vol. 369, pp. 1280 –1300, 2011.

[6] M. M. Aziz, "Sub-nonosecond electromagnetic-micromagnetic dynamic simulations using the finite-difference time-domain method," Progress in Electromagnetics Research B, vol. 15, pp. 1 –29, 2009.

[7] F. Kung and H. T. Chuah, "Stability of classical finite-difference time-domain (FDTD) formulation with nonlinear elements–a new perspective," Progress in Electromagnetics Research, vol. 42, pp. 49 –89, 2003.

[8] J. A. Kong, Electromagnetic Wave Theory. New York: John Wiley & Sons, Inc, 1990.

[9] A. D. Greenwood, K. L. Cartwright, J. W. Luginsland, and E. A. Baca, "On the elimination of numerical Cerenkov radiation in PIC simulations," J. Comput. Phys., pp. 665 –684, 2003.